Integrated CO_2 capture and reduction catalysis
Role of γ-Al_2O_3 support, unique state of potassium and synergy with copper

Pinto, Donato; Minorello, Stefano; Zhou, Zhouping; Urakawa, Atsushi

DOI
10.1016/j.jes.2023.06.006

Publication date
2024

Document Version
Final published version

Published in
Journal of Environmental Sciences (China)

Available online at www.sciencedirect.com

ScienceDirect

www.elsevier.com/locate/jes

JES JOURNAL OF ENVIRONMENTAL SCIENCES

www.jesc.ac.cn

Research Article

Integrated CO_2 capture and reduction catalysis: Role of γ-Al_2O_3 support, unique state of potassium and synergy with copper

*Donato Pinto, Stefano Minorello, Zhouping Zhou, Atsushi Urakawa**

Catalysis Engineering, Department of Chemical Engineering, Delft University of Technology, Delft, 2629HZ, Netherlands

ARTICLE INFO

Article history:
Received 31 March 2023
Revised 6 June 2023
Accepted 7 June 2023
Available online 15 June 2023

Keywords:
Carbon dioxide
Carbon capture and utilisation
CO_2 capture and reduction
Solid CO_2 sorbents
Heterogeneous catalysis
Potassium
Copper catalysts
Aluminium oxide

ABSTRACT

Carbon dioxide capture and reduction (CCR) process emerges as an efficient catalytic strategy for CO_2 capture and conversion to valuable chemicals. K-promoted Cu/Al_2O_3 catalysts exhibited promising CO_2 capture efficiency and highly selective conversion to syngas ($CO + H_2$). The dynamic nature of the Cu-K system at reaction conditions complicates the identification of the catalytically active phase and surface sites. The present work aims at more precise understanding of the roles of the potassium and copper and the contribution of the metal oxide support. While γ-Al_2O_3 guarantees high dispersion and destabilisation of the potassium phase, potassium and copper act synergistically to remove CO_2 from diluted streams and promote fast regeneration of the active phase for CO_2 capture releasing CO while passing H_2. A temperature of 350°C is found necessary to activate H_2 dissociation and generate the active sites for CO_2 capture. The effects of synthesis parameters on the CCR activity are also described by combination of *ex-situ* characterisation of the materials and catalytic testing.

Introduction

Drastic actions to abate CO_2 emissions are required in the short term to prevent global warming while transitioning towards a more carbon neutral industry and economy. Carbon capture and storage (CCS) strategies are technologically mature options to abate emissions from highly emitting sectors as industry and energy production, by CO_2 sequestration and storage in geological sites (Haszeldine et al., 2018; Marocco Stuardi et al., 2019). Current implementation of CCS strategies, however, is too slow to act as realistic solution for the abatement of CO_2 emissions (Rubin et al., 2015). The principal bottlenecks are the energy penalties and high costs associated to sorbent regeneration, compression and transportation steps. In addition, the CO_2 is essentially treated as a waste, thus CCS processes do not generate any economic return and ultimately fail to develop a closed carbon cycle.

In this regard, carbon capture and utilisation (CCU) strategies stand as favourable solutions to recover the captured CO_2 and valorise it as a feedstock for production of more carbon neutral chemical and fuels (Aresta et al., 2014; Fernández et al., 2020; Leclaire and Heldebrant, 2018). Despite its abundance, CO_2 utilisation in chemical industry is scarce due to its thermodynamic stability and relative inertness. A half of the CO_2

* Corresponding author.
E-mail: A.Urakawa@tudelft.nl (A. Urakawa).

https://doi.org/10.1016/j.jes.2023.06.006
1001-0742/

utilised as feedstock in industry is used in urea synthesis, but it is also employed in synthesis of carboxylic acids, in the CO hydrogenation to methanol and as an additive in food industry. However, these applications currently utilise a limited amount of CO_2, less than 1% of the CO_2 emitted every year from anthropogenic sources (Mikkelsen et al., 2010).

In order to extend the utilisation of CO_2 as feedstock, it is desirable to convert it into more reactive C1 building blocks (e.g., CO, CH_4, CH_3OH), which can be exploited in existing industrial processes (Keim, 1986). However, methanol synthesis and reverse water-gas shift to CO suffer from thermodynamic limitation, requiring harsh conditions (temperature, pressure) to obtain adequate conversions, while exothermic methanation is favoured at low temperature where yields are kinetically limited (Cui and Kær, 2019; Stangeland et al., 2017). Moreover, conventional catalytic processes put a strong requirement on the purity and compression of the CO_2 feedstock, incrementing the total costs and energy requirements.

In this perspective, strategies that combine the capture of CO_2 from diluted sources with its conversion to valuable chemicals are effective solutions to decrease the energy penalty associated with the purification and pressurisation steps (Marocco Stuardi et al., 2019; Zhang et al., 2022). Aiming at one-step capture and conversion of CO_2, a new CCU strategy referred to as 'integrated CO_2 capture and conversion' or 'CO_2 capture and reduction' (CCR) was recently demonstrated. This approach effectively integrates in one process the sequestration of CO_2 from diluted streams (e.g. flue gases, air) with its conversion to more valuable molecules as CO and CH_4. Farrauto group proposed a bifunctional catalyst materials based on Ru and CaO with the ability of capturing CO_2 and converting it to CH_4 by use of green H_2 (Duyar et al., 2015). Urakawa group demonstrated the activity of catalysts made of earth-abundant elements in terms of CO_2 capture efficiency and selective conversion to syngas ($CO + H_2$) (Bobadilla et al., 2016; Hyakutake et al., 2016). The overall reaction can be thought as a reverse water-gas shift reaction (RWGS) performed in an unsteady-state operation. A CO_2-containing feed is sent to the catalytic bed for CO_2 capture followed by a H_2 feed that reduces the captured CO_2 and releases it as CO. Thanks to the reversibility of the sorption, the capture and reduction processes are operated at same temperature and pressure, eliminating the need of sorbent (catalyst) regeneration step and potentially lowering energy requirements. Moreover, continuous CCR operation with excellent performances can be obtained in circulating fluidised bed reactors. A recent publication (Kosaka et al., 2022) demonstrated that CO_2 can be captured from low concentration feed (2%) and converted into high concentration CH_4 stream (20%) with high capture efficiency and H_2 conversion.

Bifunctional catalyst materials exhibiting the abilities to capture CO_2 from flue gas and selectively convert it to the desired product are needed (Duyar et al., 2015). CaO is well-known for the CO_2 capture ability through carbonation reaction, but it needs high temperature for regeneration and generally shows poor stability over the capture-regeneration cycles (Abanades, 2002; Shimizu et al., 1999). It has been reported that other alkali/alkaline-earth metals (Li, Na, K, Cs, Ba) are effective promoters, increasing the CO_2 sorption capacity of the base materials (Arco et al., 1989; Cimino et al., 2020; Hyakutake et al., 2016; Oliveira et al., 2008; Roesch et al., 2005). Amongst them, K shows unique promotion properties by ensuring highly efficient CO_2 capture and reactive desorption of captured CO_2 to CO under H_2 atmosphere at isothermal conditions in the temperature range of 300–500°C (Bobadilla et al., 2016; Lee et al., 2010; Walspurger et al., 2008). Besides the alkali promoter, the introduction of transition metals in the catalytic systems is fundamental to ensure the conversion of the captured CO_2. The choice of the active metal greatly affects the reduction products. The use of Ni or Ru promotes catalytic methanation (Duyar et al., 2015; Hu and Urakawa, 2018; Kosaka et al., 2021) of the captured CO_2, while Cu brings high selectivity towards CO (Bobadilla et al., 2016; Hyakutake et al., 2016). The latter case is attractive for the versatility of the technology and product, since the presence of product CO and unconverted H_2 during the reduction phase results in the production of a syngas, with H_2/CO ratio tuneable by changing operation conditions and further adding H_2 in the product stream.

Considering the relevance of designing efficient catalytic systems, it is fundamental to understand the catalytic role of the different promoters and their participation in the CCR process. In reaction conditions, the two functionalities interplay in a highly dynamic system. In a previous attempt to elucidate the role of K and its interaction with Cu by means of *operando* XRD analysis (Hyakutake et al., 2016), it was reported that the generation of a highly dynamic state in reaction conditions, with a profound change in the crystalline structure of the material. However, the dynamic nature of the catalyst and catalytic process set the barrier high for detailed investigations on the roles of K and its synergistic interaction with Cu. Another question mark regards the role of the support material and its contribution to the CCR activity. Studies about the influence of support material on the mechanism of RWGS reaction led to the distinction between irreducible oxides (Al_2O_3, SiO_2) promoting activation of CO_2 via formate route and reducible oxides (TiO_2, CeO_2) activating CO_2 through oxygen vacancies (Zhu et al., 2020). Employment of γ-Al_2O_3 and MgO-Al_2O_3 mixtures as supports ensured high CCR performance in various catalytic systems (Arellano-Treviño et al., 2019; Bobadilla et al., 2016; Kosaka et al., 2021). Modification of Al_2O_3 with basic metal oxides is known to increase the heat of CO_2 adsorption and, in particular, a strong interaction between the acidic γ-Al_2O_3 support and the basic K_2CO_3 is expected (Kantschewa et al., 1983). Hu and Urakawa (2018) reported activity in integrated CO_2 capture and methanation for a ZrO_2-supported catalyst. However, their role as supports in bifunctional catalysts for integrated CO_2 capture and conversion have not been clarified yet.

In this work, we employed K-promoted Cu/γ-Al_2O_3 catalysts as the model system to identify the fundamental catalytic properties to develop the CCR activity. Catalysts with variable composition were prepared and tested to elucidate the roles of potassium promotion and of the Cu active metal as well as their synergetic behaviour to develop efficient CO_2 capture and selective reduction to CO. Synthesis parameters, including the choice of the potassium precursors and the conditions of the impregnation synthesis, were evaluated to clarify their influence on the formation of the active CCR phase. Besides, the peculiarities of the γ-Al_2O_3 as support

were investigated in comparison to TiO_2 rutile and ZrO_2 counterparts. Temperature-dependant catalytic activity was studied to identify the conditions for the formation of the catalytically active phase for CCR. The empirical evidences collected in this work suggest that an highly amorphous state of potassium, whose formation is favoured by high dispersion on the γ-Al_2O_3 support, interacts with the metallic Cu phase to synergistically develop the unique CCR catalytic activity.

1. Materials and methods

1.1. Catalyst synthesis

Aluminium oxide (γ-phase, Alfa Aesar, catalyst support), titanium oxide (rutile, Alfa Aesar, > 99.5%) and zirconium oxide (monoclinic, Alfa Aesar, catalyst support) were employed as support material. Cu and K were introduced by incipient wetness impregnation using copper nitrate trihydrate (Merck Sigma, > 99.5%) and potassium carbonate anhydrous (Merck Sigma, > 99.0%) as precursors. Potassium nitrate (ACS reagent, Merck Sigma, > 99.0%) and potassium bicarbonate (Merck Sigma, > 99.5%) were also employed as potassium precursors. A two-step impregnation procedure was used. First, the support material was impregnated with the aqueous solution of copper nitrate, dried overnight at 80°C and calcined at 500°C for 5 hr in air. Then, the resulting catalyst was further impregnated with an aqueous solution of the potassium precursor, followed again by overnight drying at 80°C and calcination at 500°C for 5 hr in air.

1.2. Catalyst characterisation

Powder X-ray diffractograms were acquired on a Bruker D8 Advance diffractometer with Bragg-Brentano geometry using monochromatic Co Kα radiation (λ = 1.7902 Å) or Cu Kα radiation (λ = 1.5405 Å). BET surface area of the catalysts was determined from N_2 adsorption isotherms at 77 K using a Micromeritics TriStar II 3020 instrument. H_2 temperature programmed reduction (H_2-TPR) was carried out in a dedicated set-up, consisting of a tubular furnace in which a 6 mm internal diameter quartz tube for holding the sample is inserted and equipped with thermal conductivity detector (TCD) to monitor H consumption. Experiments were performed using a diluted H_2 stream (10 vol.% in Ar) with a 30 mL/min flow rate. 100 mg of sample were charged in the tube, and its temperature was raised from 25 to 800°C with a ramp rate of 10°C/min. Scanning electron microscopy and energy dispersive X-ray spectroscopy (SEM-EDS) measurements were carried out on a JEOL JSM-6010LA *InTouchScope* operated in high vacuum mode, with acceleration voltage set at 20 kV. Transmission electron microscopy was carried out on a Jeol JEM1400 plus TEM.

1.3. Catalytic reaction

The catalytic testing was carried on a dedicated set-up, in a configuration similar to the one reported in previous works (Hyakutake et al., 2016). A schematic representation of the reaction set-up is presented in Appendix A Fig. S1. The inlet feed was controlled by a system of mass flow controllers (MFCs, Bronkhorst) and two electric 4-way valves to switch amongst different gas flows at the inlets. The reactor consisted of a tubular quartz tube reactor (4 mm ID, 6 mm OD), loaded with 200 mg of catalyst material, pelletized, crushed and sieved in 200–300 µm range. Prior to each reaction, the catalyst underwent an activation treatment consisting of 50 mL/min of pure H_2 at 450°C for 1 hr. The temperature of the bed was controlled by a thermocouple inserted in the quartz reactor. The catalytic performance was evaluated under CCR conditions at different temperatures (300, 350, 400 and 450°C) and ambient pressure. A typical reaction cycle consisted of the alternation of 25 mL/min of 10 vol.% CO_2 in He, to a reduction phase consisting of 50 mL/min of H_2 (100 vol.%). An inert phase of He (80 mL/min, 100 vol.%) was flushed between the CO_2 and H_2 phases (and vice versa). The composition of the product gas mixture was evaluated quantitatively by Fourier transform infrared (FTIR) spectroscopy (ALPHA Bruker) with a time resolution of 5 s. Valve switching and spectral acquisition were synchronised by LabView software. The data presented resulted from the average of multiple cycles of stable operation, after a reproducible activity was achieved.

Quantitative comparison of the CCR activity of different catalyst was made on the basis of the capture capacity defined by Eq. (1):

$$\text{Capture capacity} = \int (CO)/g_{cat} \quad (1)$$

as the total amount of CO released during the reducing H_2 pulse per gram of catalyst (g_{cat}) expressed in µmol/g (Kosaka et al., 2021).

2. Results and discussion

CO_2 capture and reduction was performed experimentally by exposing the catalytic bed to the periodic alternation of a diluted CO_2 feed (10 vol.% in He) and pure H_2. The gas composition of the reactor outlet stream was analysed by FTIR. The gaseous concentration profile for a blank CCR experiment is reported in Fig. 1. Each CCR cycle of operation consisted of a CO_2 pulse (0–420 sec), followed by the reducing H_2 pulse (570–990 sec). For the purposes of this investigation, inert flushing phases (He, 420–570 sec and 990–1140 sec) were introduced between the CO_2 and H_2 pulses to avoid mixing of the reactants phases, to eliminate possible side reactions activated in co-feed conditions and to univocally identify the role of the catalytic materials in the capture and reduction phases.

2.1. Catalytic role of potassium

Bifunctional materials guarantee the activity in CO_2 capture and reduction reactions (CCR), introducing both the strong affinity to CO_2 and the selectivity towards the desired carbon products. Following the previous contribution (Hyakutake et al., 2016), we employed a Cu-K/Al_2O_3 catalyst (Cu 11 wt.%, K 10 wt.%) as a model system to investigate the catalytic roles of the two promoters.

The X-ray diffractograms acquired on the synthesised materials are reported in Appendix A Fig. S2. Potassium would

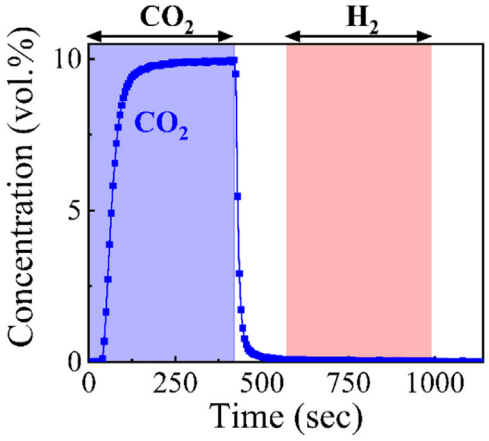

Fig. 1 – Reactor outlet CO_2 concentration obtained by FTIR spectroscopy during a blank CCR experiment on a Cu-K/Al_2O_3 catalyst (11 wt.% Cu, 10 wt.% K) at room temperature. CCR cycle consists of the alternation of diluted CO_2 feed (blue region, 25 mL/min, 10 vol.% in He, 0–420 sec), He flush (50 mL/min, 420–570 sec), pure H_2 feed (red region, 50 mL/min, 570–990 sec), He flush (50 mL/min, 990–1140 sec).

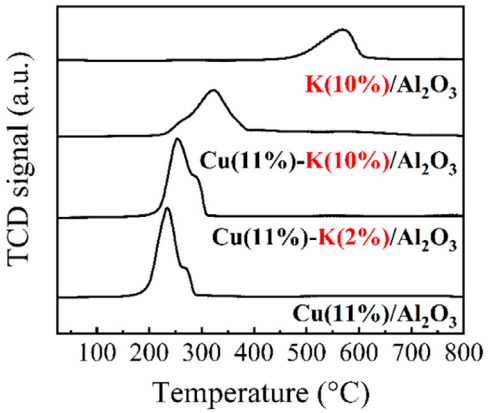

Fig. 3 – H_2-TPR profiles of γ-Al_2O_3 supported catalysts. Sample were treated under H_2 flow (10 vol.% in Ar, 30 mL/min) and heating rate of 10°C/min.

be expected in the carbonate form, considering its employment as precursor for the synthesis and the calcination performed in air. However, no K_2CO_3 reflexes were detected. Similar results were previously reported (Bansode et al., 2013), pointing out the existence of a highly dispersed K phase in the form of nanocrystallites or thin layers. The appearance of narrow metallic Cu reflexes in the XRD reflects a sintering phenomenon, indicating that the amount of copper employed exceeds the conditions to obtain a uniform dispersion of nanocrystals.

To isolate the promotional effect of potassium, we compared the catalytic performance of the catalysts at increasing potassium loadings (Fig. 2). Fig. 2a shows that the unpromoted catalyst (11 wt.% Cu / Al_2O_3) does not possess the ability to capture CO_2. During the CO_2 pulse, CO was produced from the direct interaction with the reduced catalyst. No CO_x species were released in the H_2 pulse, indicating that the capture of CO_2 is not active in absence of potassium. Low loadings of potassium are not sufficient to develop the active phase for CO_2 capture, as indicated by the results obtained in Fig. 2b for a K-promoted Cu/Al_2O_3 catalyst (11 wt.% Cu, 2 wt.% K). However, the presence of potassium undermined the CO_2 reduction responsible for CO produced in the CO_2 pulse, indicating an interaction between the copper and potassium phases. At higher loading of K (10 wt.% K, 11 wt.% Cu), the emergence of the typical CCR catalytic activity was noticed (Fig. 2c). CO_2 was sequestrated from the feed, and then selectively converted and released as CO in the H_2 pulse. No other carbon-containing products were detected within the detection limit. The results indicated that an optimum loading of potassium exists and high CCR catalytic activity may be obtained when particular conditions of high dispersion of potassium phase and intimate contact with copper are fulfilled.

To gain insights into the interaction between Cu and K phase in the catalytic system, H_2 temperature programmed reduction (H_2-TPR) analysis was conducted (Fig. 3). For the unpromoted Cu/Al_2O_3 catalyst, complete Cu(II) reduction to metallic Cu(0) is achieved at 300°C. The profile presents a main peak at around 235°C with a small shoulder centred at around 270°C. The first peak can be assigned to the presence of highly dispersed CuO nanoparticles, while the shoulder can be related to bulk oxidation of bigger agglomerates (Luo et al., 2014).

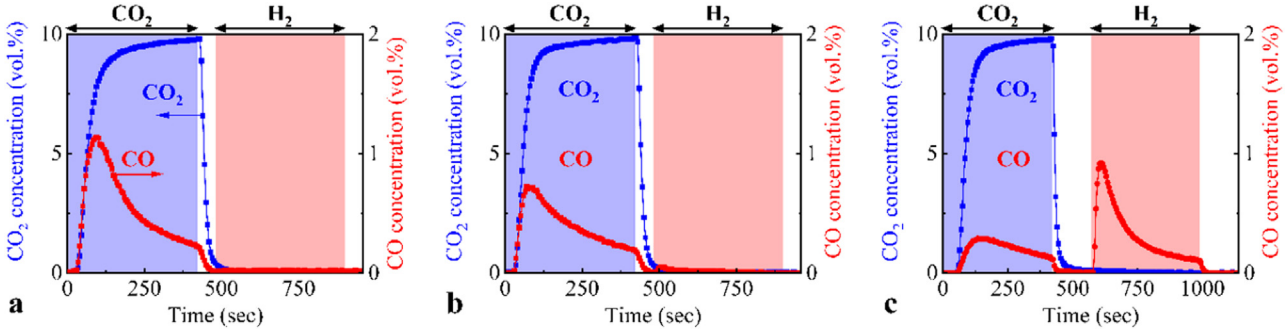

Fig. 2 – Concentration profiles of CO_2 (blue) and CO (red) during CCR at 350°C, 1 bar with 10% CO_2 in He (blue region) at 25 mL/min vs. 100% H_2 (red region) at 50 mL/min over a) Cu/Al_2O_3 (Cu 11 wt.%), b) Cu-K/Al_2O_3 (Cu 11 wt.%, K 2 wt.%), c) Cu-K/Al_2O_3 (Cu 11 wt.%, K 10 wt.%). He flush phase at 80 mL/min in between the CO_2 and H_2 pulses.

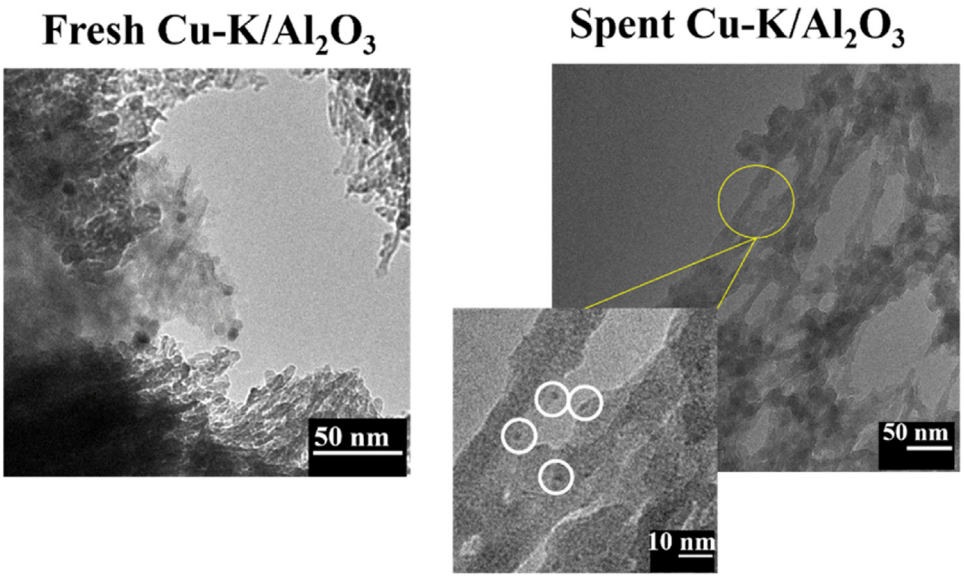

Fig. 4 – TEM images for the Cu-K/Al_2O_3 (Cu 11 wt.%, K 10 wt.%) fresh (left) and spent after 50 CCR cycles at 350°C (right).

Compared to the unpromoted Cu/Al_2O_3 catalyst, the reduction peak of CuO shifted towards higher temperatures in presence of potassium, from ca. 235°C to 325°C in case of 10 wt.% K loading. Conversely, the decomposition of K_2CO_3 was enhanced at lower temperatures thanks to the formation of metallic Cu. In fact, the reduction profile peaked at around 570°C observed for the K/Al_2O_3 catalyst (10 wt.% K) was lost in the catalyst containing Cu in favour of a wide reduction shoulder between 390 and 690°C detected in the Cu-K/Al_2O_3 system (10 wt.% K, 11 wt.% Cu).

The decomposition of K_2CO_3, a crucial step for the activation of the catalyst towards CO_2 capture, can be depicted as the results of a dynamic interplay of reactions. When the catalyst is exposed to H_2 feed and heated, the reduction of CuO produce H_2O (Eq. (2)). The resulting metallic Cu activates the H_2 molecule (Eq. (3)), making H species available on the catalyst surface ($H_{(ads)}$) (Christmann, 1995). It has been reported that the K_2CO_3 decomposition (Eq. (4)) is significantly enhanced in presence of water release from CuO reduction (Eq. (5)) (Duan et al., 2012). This is confirmed by the TPR profiles of Fig. 3, where the reduction of the K_2CO_3 phase in the Cu-containing catalysts is promoted at lower temperatures compared to the K/Al_2O_3 system. When the CuO is fully reduced, as in CCR reaction conditions, H species from H_2 dissociation on metallic copper can drive K_2CO_3 decomposition further. *Operando* DRIFTS results suggest that, in CCR conditions, a KOH phase can be generated by interaction of the K_2CO_3 with adsorbed H species (Eq. (6)) (Pinto et al., 2022).

$$CuO + H_2 = Cu + H_2O_{(g)} \quad (2)$$

$$Cu + H_2 = Cu + 2H_{(ads)} \quad (3)$$

$$K_2CO_3 = K_2O + CO_2 \quad (4)$$

$$K_2CO_3 + H_2O = 2KOH + CO_2 \quad (5)$$

$$K_2CO_3 + 2H_{(ads)} = 2KOH + CO \quad (6)$$

During the catalyst activation step in H_2, the reduction of CuO triggers the decomposition of K_2CO_3 initially as an effect of water release and then by continuous supply of H species from dissociation of gaseous H_2 on metallic Cu. Cu and K phases interact strongly in reaction conditions. *In situ* XRD measurements on a similar system (Hyakutake et al., 2016), revealed that in reaction conditions a highly dynamic state is generated, with a profound change in the crystalline structure. In such state, the absence of crystalline CuO or metallic Cu reflexes was noticed and addressed to a nanodispersion of the Cu phase induced by the contact with the highly dynamic K phase. Transmission electron microscopy images collected for the Cu-K/Al_2O_3 catalyst (10 wt.% K, 11 wt.% Cu) after 50 CCR cycles at 350°C, shown in Fig. 4 (catalytic results in Appendix A Fig. S3), support the previous observation. While CuO nanoparticles up to 10 nm diameter are clearly observed in the fresh sample, small dispersed Cu nanoparticles (2–3 nm) are observed in the sample after reaction condition. A similar behaviour was reported on a K-promoted Pt/Al_2O_3 (Luo et al., 2014), for which they related the formation of finely dispersed Pt species under thermal ageing to the interaction with an extremely mobile K phase. Preliminary investigation by in situ soft-X-ray absorption spectroscopy (Appendix A Fig. S4-S6) also revealed a change in the state of K in reaction conditions possibly due to the generation of a highly disordered potassium phase with increased dispersion on the γ-Al_2O_3 support. Such high dispersion and the intimate contact between the metallic Cu and the K phase are expected to play a key role for the activity of the catalyst towards CCR.

2.2. *Influence of synthesis conditions*

The extremely dynamic nature of the catalytic system in reaction conditions challenges the identification of the potassium active phase for developing CCR catalysis. The nature

of this potassium phase, however, is independent of the K precursor employed in the synthesis. In this work, three Cu-K/Al_2O_3 catalysts (Cu 10 wt.%, K 10 wt.%) were synthesized employing different K precursors, namely potassium carbonate, bicarbonate and nitrate. Those salts were chosen in view of their different thermal stability. Bulk KNO_3 decomposition is reported at temperatures higher than the calcination temperature of 500°C employed in this work (Gordon and Campbell, 1955; Udupa, 1976), while $KHCO_3$ starts decomposing to K_2CO_3 already at temperatures as low as 100°C (Hartman et al., 2019).

Interestingly, though the as-synthesized materials exhibited some differences in terms of structural and morphological properties (Appendix A Table S1), the CCR activity was preserved and similar catalytic behaviour was observed for all the samples. Catalytic activity (Appendix A Table S1 and Fig. S7) indicated that the active K phase was generated in reaction conditions for all the catalysts, independently of the K precursor employed during the synthesis. The results suggest that, during catalyst activation and CCR reaction, a similar potassium state was generated for all the samples. Such indication was confirmed by the X-ray diffractograms of the spent samples (Appendix A Fig. S8), that showed comparable patterns after CCR reaction.

The potassium-derived catalytically active phase is crucial in the generation of CO_2 capture and reduction activity, thus it appears meaningful to investigate its dependence on synthesis conditions. To this scope, we synthesized and tested 4 different Cu-K/Al_2O_3 (Cu 11 wt.%, K 10 wt.%). Each catalyst was synthesized using an increasing amount of water in the potassium impregnation step, with the objective of transitioning from the incipient wetness impregnation regime to conditions closer to wet impregnation synthesis. For incipient wetness impregnation synthesis, the volume of potassium precursor solution matches the pore volume of the powder to be impregnated (defined here as 1 unit of pore volume). In this case, capillary forces drive the solution inside the pores maximising the dispersion of K.

Employing an excess of water (2, 3 and 5 units of pore volume in this work) in the impregnation, the deposition of the solute inside the material pores is expected to be mainly governed by diffusional forces, requiring longer times to achieve an equilibrium composition (Marceau et al., 2009). X-ray diffractograms of the samples showed similar patterns Appendix A Fig. S9). Only low intensity broad reflexes associated to dispersed CuO nanocrystallites and the γ-Al_2O_3 support were detected. The absence of K-related reflexes confirmed the low crystalline character of the phase. SEM-EDX composition analysis (Appendix A Table S2) suggested that excess of water in the K impregnation leads to a lower concentration of potassium in the catalyst bulk, preventing uniform dispersion and possibly favouring surface segregation of the potassium phase. Both BET surface area and pore volume of the catalysts increased with the amount of water employed in the potassium impregnation step, indicating that, approaching wet impregnation synthesis conditions, pore filling with the potassium solution and deposition of the potassium phase were avoided (Appendix A Table S3). Fig. 5 shows the performance of the different catalysts in terms of CO_2 capture capacity, as defined in the Materials and Methods section (Eq. (1)).

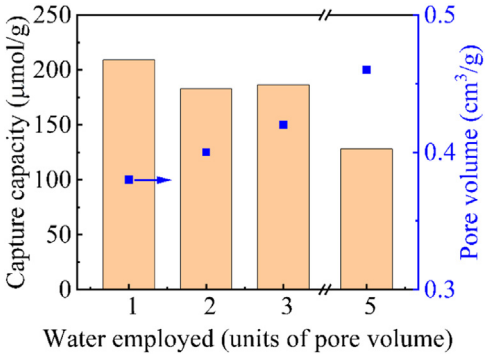

Fig. 5 – Capture capacity and pore volume for Cu-K/Al_2O_3 (Cu 10 wt.%, K 10 wt.%) synthesized with different amount of water in potassium impregnation step (1–5 × pore volume of support).

The employment of excess water in the K impregnation step undermined the activity of the Cu-K/Al_2O_3 catalysts. The reproducibility of the synthesis procedure was tested, and the catalytic activity results were confirmed (Appendix A Table S4), with the descending trend of capture capacity at increasing water amount in the K impregnation. The catalyst prepared with incipient wetness impregnation (i.e. 1 unit of pore volume of water solution) showed the highest performance, indicating that, besides exhibiting lower surface area and pore volume, the uniform dispersion of potassium and the maximisation of contact with the copper phase are decisive properties to maximise CCR activity.

2.3. *Catalytic role of copper*

The role of transition metals in bifunctional materials for the integrated capture and conversion of CO_2 is promoting the reduction of the captured CO_2 and selectively driving its conversion towards the desired products (CO or CH_4). Copper, especially, is known to provide high selectivity towards CO_2 conversion to CO. For this reason, Cu-based catalysts are frequently employed for CO_2 reduction reactions, as the reverse water-gas shift (RWGS) (Porosoff et al., 2016). Reduced copper species are reported to dissociate gaseous H_2 and provide active H species that increase the reducibility of CO_2 and selectively form CO (Chen et al., 2000; Ernst et al., 1992). In this section, we investigate the role of copper in the development of the CO_2 capture and reduction activity.

A K/Al_2O_3 catalyst (K 10 wt.%) was synthesized to investigate the catalytic behaviour in absence of copper. The activation pretreatment of the catalyst in H_2 (1 hr at 450°C) leads to the decomposition of the K phase generating active sites for capture. After that, capture of CO_2 from the feed was noticed during the first cycle of CCR operation at 350°C (Appendix A Fig. S10). However, the regeneration of the active phase is kinetically slow at reaction temperature and the short duration of the H_2 pulse in operating conditions (420 sec) prevented the full regeneration of the catalyst after the first cycle. As shown in Fig. 6a, the ability to capture CO_2 was drastically abated in the following reaction cycles and continuous CCR activity could not be achieved. In absence of copper, only a limited por-

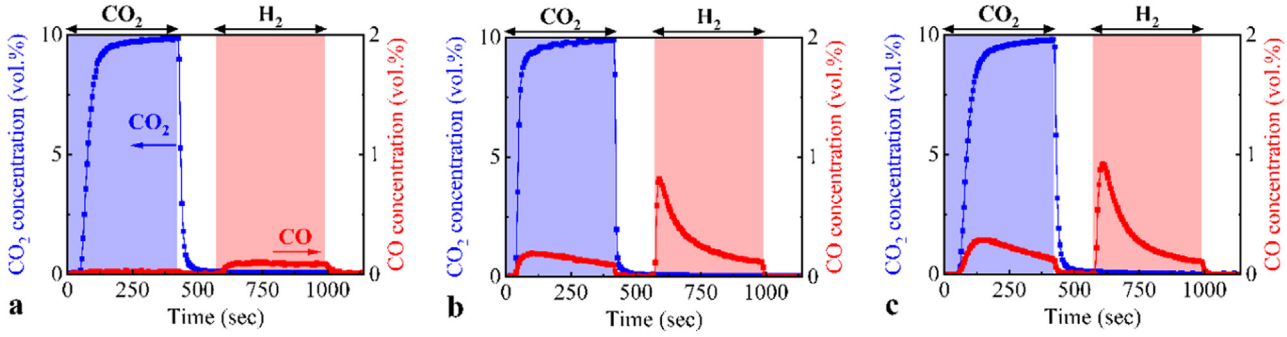

Fig. 6 – Concentration profiles of CO_2 (blue) and CO (red) during CCR at 350°C, 1 bar with 10% CO_2 in He (blue region) at 25 mL/min vs. 100% H_2 (red region) at 50 mL/min over (a) K/Al_2O_3 (K 10 wt.%), (b) Cu-K/Al_2O_3 (Cu 1 wt.%, K 10 wt.%), (c) Cu-K/Al_2O_3 (Cu 11 wt.%, K 10 wt.%). He flush phase at 80 mL/min in between the CO_2 and H_2 pulses.

tion of the potassium phase can be decomposed at low reaction temperature. As a consequence, the catalyst exhibits very low CO_2 capture capacity (65.5 µmol/g).

A substantial enhancement of the activity in reduction of captured CO_2 was obtained already at low Cu loadings (Cu 1 wt.%, K 10 wt.%), as shown in Fig. 6b. During the H_2 pulse (570–990 sec), the high release of CO indicates that kinetic of reduction was clearly boosted, resulting in a drastic improvement of CCR performance in terms of CO_2 capture capacity (210.2 µmol/g). Metallic copper introduced the selective reduction of the captured CO_2 and promoted fast regeneration of the active phase for capture, key properties to develop isothermal cyclic CCR operation. H species generated by H_2 activation on Cu appear to be decisive for the decomposition of the potassium phase and the selective release of CO.

Fig. 6c shows that increasing the loading of copper (Cu 11 wt.%, K 10 wt.%) does not play a decisive role in enhancing the performance of the catalytic system, since only a minor increase in capture capacity was detected (227.5 µmol/g). More than the absolute loading of copper, a decisive role seems to be played by the dispersion of K and Cu and the optimal contact between the two phases at reaction conditions. In analogy with a proposed mechanism for RWGS reaction (Porosoff et al., 2016), the close contact between the phases may favour the spillover of H species from the metallic copper to the capture sites, providing the reduction of CO_2 to CO (Conner and Falconer, 1995).

2.4. *Contribution of metal oxide support to ccr catalysis*

In the previous sections, the role of Cu and K in the development of the CO_2 capture and reduction catalysis has been elucidated. In the attempt of determining the role of the metal oxide support in generating the catalytically active phase for CCR, we investigated the reaction on similar Cu-K catalytic systems supported on TiO_2 (rutile) and ZrO_2 (Cu 10 wt.%, K 10 wt.%). XRD of the catalysts are reported in Appendix A Fig. S11. The catalytic activity results are shown in Fig. 7. Negligible activity in CO_2 capture is noticed for the TiO_2-supported catalyst, as reflected in the low amount of CO evolved in the H_2 pulse. The formation of a K-Ti mixed oxide phase, which is stable in reaction conditions, may explain the inability of the catalyst of generating an active potassium state for CO_2 capture (Appendix A Fig. S11). Although showing some activity, the ZrO_2-supported catalyst performed significantly worse than its γ-Al_2O_3-based counterpart (Fig. 2c). Appendix A Fig. S12 reports the CO_2 capture capacities of the three catalytic systems measured at 350°C and their BET surface area. The results suggest that, thanks to its high surface area, γ-Al_2O_3 support markedly enhances the CCR activity ensuring adequate dispersion of the Cu nanoparticles and maximizing the contact between Cu and K phases.

Comparing different support materials employed for RWGS reaction, high dispersion of Cu on Al_2O_3 and ZrO_2 was found on catalysts prepared by deposition precipitation method, with Cu/Al_2O_3 exhibiting the highest catalytic activity (Jurković et al., 2017). Relations between the catalytic activity and the acidity of metal oxides should also be considered. γ-Al_2O_3 exhibit strong Lewis acid sites while weaker acidity is found for the amphoteric TiO_2 and ZrO_2 (Álvarez et al., 2017; Ferretto and Glisenti, 2003; Lahousse et al., 1993). The added potassium promoter is known to strongly interact with acidic supports (Bansode et al., 2013; Garcia Cortez et al., 2003), causing their neutralisation. In this sense, the acidity of γ-Al_2O_3 can promote a peculiar interaction with the K_2CO_3. The fine dispersion and the strong interaction with Al_2O_3 have been shown to enhance the K_2CO_3 decomposition at lower temperatures in comparison with bulk K_2CO_3 (Kantschewa et al., 1983; Walspurger et al., 2008), as also detected in the TPR results of Fig. 3. Such increased destabilisation of the K_2CO_3 phase helps to generate the potassium active state for CO_2 capture and reduction.

2.5. *Temperature and generation of the catalytically active phase*

Fig. 8 reports the catalytic activity results obtained for the Cu-K/Al_2O_3 catalyst (Cu 11 wt.%, K 10 wt.%) in four different experiments at varying reaction temperatures. Looking at the catalytic behaviour, the typical CCR activity was noticed starting from a temperature of 350°C. A significant change in the reduction mechanism was observed at this temperature. The higher CO formation detected at 350°C during both CO_2 and H_2 pulses revealed an enhancement of direct CO_2 hydrogenation and captured CO_2 reduction, respectively. The results indicate that a temperature of 350°C is decisive for the formation of the

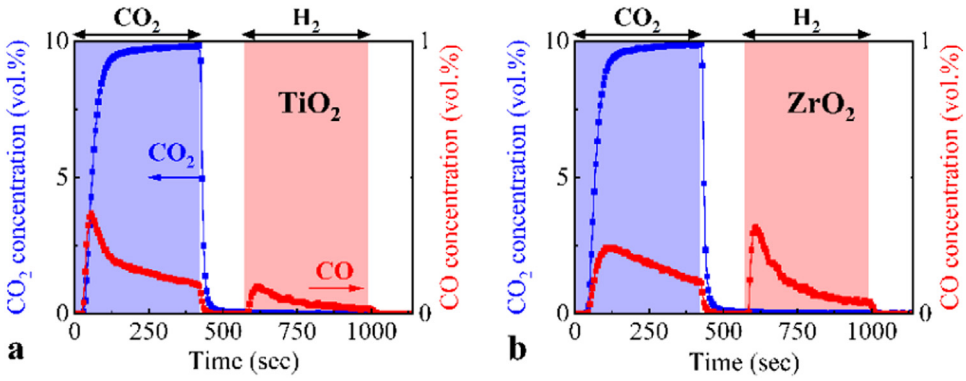

Fig. 7 – Concentration profiles of CO_2 (blue) and CO (red) during CCR at 350°C, 1 bar with 10% CO_2 in He (blue region) at 25 mL/min vs. 100% H_2 (red region) at 50 mL/min over a) Cu-K/TiO_2 (Cu 10 wt.%, K 10 wt.%) and b) Cu-K/ZrO_2 (Cu 10 wt.%, K 10 wt.%). He flush phase at 80 mL/min in between the CO_2 and H_2 pulses.

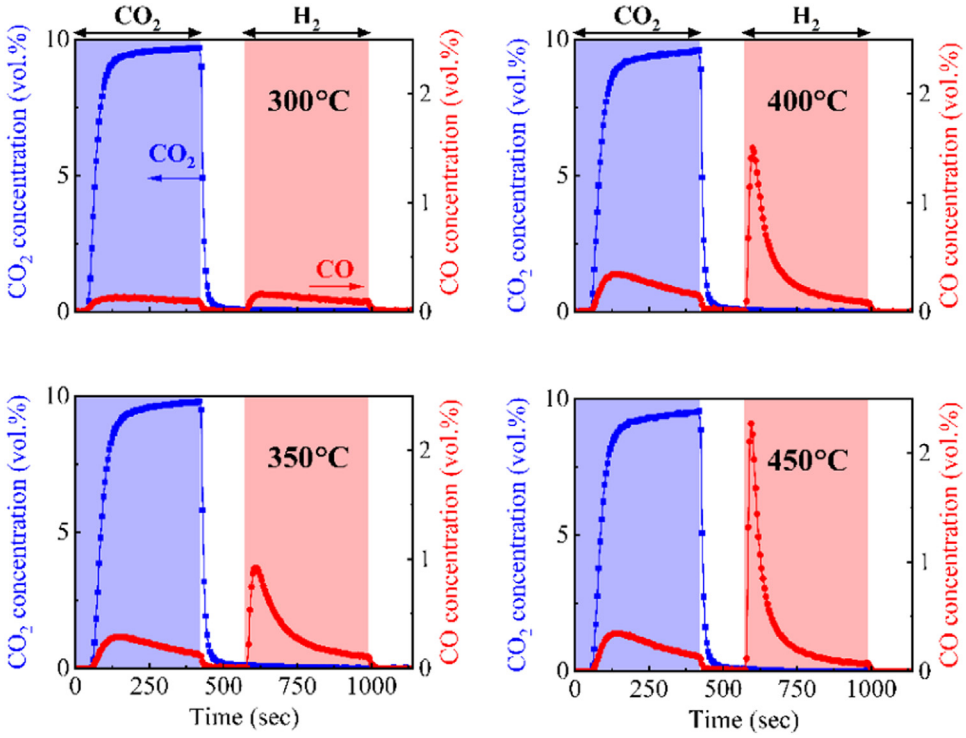

Fig. 8 – Concentration profiles of CO_2 (blue) and CO (red) during CCR at 350°C, 1 bar with 10% CO_2 in He (blue region) at 25 mL/min vs. 100% H_2 (red region) at 50 mL/min over Cu-K/Al_2O_3 (Cu 11 wt.%, K 10 wt.%) at different reaction temperatures. He flush phase at 80 mL/min in between the CO_2 and H_2 pulses.

active phase for CO_2 capture and reduction in the Cu-K/Al_2O_3 system. The TPR profiles of Fig. 3 also displayed an increased H_2 consumption in this temperature range, assignable to both CuO reduction and K_2CO_3 decomposition. In reaction conditions, with the copper already in its metallic state, 350°C is necessary to activate H_2 dissociation (Rodriguez et al., 2003). At this temperature, the increased availability of surface H species promotes the decomposition of the potassium phase generating the catalytically active state for CO_2 capture. At higher temperatures, a kinetic enhancement of the CO_2 reduction was registered, in agreement with the endothermic nature of the reaction and in similarity with the RWGS (Daza and Kuhn, 2016). As a result, the CO_2 capture capacity of the catalyst increased with temperature and the profiles of CO release in the H_2 pulse exhibited a higher and narrower initial peak. From the point of view of the process development, temperature stands out as a key operating parameter to control the duration of the CO_2 and H_2 pulses. Higher temperatures can in fact shorten the H_2 pulse for regenerating the catalyst and at the same time, by concentrating the CO release in time, can tune the H_2/CO ratio in the syngas product to flexibly target the needs of the downstream processes.

3. Conclusions

The activity towards CO_2 capture and selective reduction to CO derives from a complex interaction between the Cu and K promoters and the γ-Al_2O_3 support. Potassium introduces the CO_2 affinity, but its intimate interaction with the metallic Cu is vital to generate the active phase for capture. The γ-Al_2O_3 excels as catalyst support, providing high surface area end ensuring high dispersion of potassium and intimate contact with the Cu phase. A strong interaction between the acidic sites of γ-Al_2O_3 and the basic potassium carbonate enhances the decomposition of the potassium-derived phase, generating active sites for CO_2 capture. The formation of the active phase for CO_2 capture was found to be independent of the type of potassium precursor employed in the synthesis. However, the high dispersion and intimate contact between copper and potassium phases proved to be key parameters for the activity towards CCR. The generation of active capture sites, in the H_2 pulse, was found to be activated at a temperature between 300 and 350°C in presence of copper. Metallic Cu activates H_2 dissociation and provides H species that enhance the decomposition of the potassium phase. In such a dynamic state, the synergy between Cu and K permits to aggressively capture CO_2 from the feed and selectively releasing CO when exposed to H_2, providing at the same time fast regeneration of the CO_2 capture active sites. These results furnish insights for improved catalyst design of bifunctional catalysts for integrated CO_2 capture and reduction processes.

Declaration of Competing Interest

The authors declare that they have no known competing financial interests or personal relationships that could have appeared to influence the work reported in this paper.

Acknowledgments

Part of this work was conducted in the PHOENIX I (X07MB) beamline of the Swiss Light Source, Paul Scherrer Institut, Villigen PSI, Switzerland. We acknowledge Dr. Thomas Huthwelker, Dr. Camelia Nicoleta Borca and Reto Wetter for the technical support.

Appendix A Supplementary data

Supplementary data associated with this article can be found in the online version at doi:10.1016/j.jes.2023.06.006.

References

Abanades, J.C., 2002. The maximum capture efficiency of CO_2 using a carbonation/calcination cycle of CaO/$CaCO_3$. Chem. Eng. J. 90, 303–306.

Álvarez, A., Bansode, A., Urakawa, A., Bavykina, A.V., Wezendonk, T.A., Makkee, M., et al., 2017. Challenges in the Greener production of Formates/Formic Acid, Methanol, and DME by Heterogeneously Catalyzed CO_2 Hydrogenation Processes. Chem. Rev. 117, 9804–9838.

Arco, Md, Hernández, E., Martín, C., Rives, V., 1989. Formation and evolution of Carbonate Species in Na-Doped Al_2O_3 and V_2O_5-Al_2O_3. Spectrosc. Lett. 22, 1183–1191.

Arellano-Treviño, M.A., Kanani, N., Jeong-Potter, C.W., Farrauto, R.J., 2019. Bimetallic catalysts for CO_2 capture and hydrogenation at simulated flue gas conditions. Chem. Eng. J. 375, 121953.

Aresta, M., Dibenedetto, A., Angelini, A., 2014. Catalysis for the valorization of exhaust carbon: from CO_2 to chemicals, materials, and fuels. technological use of CO_2. Chem. Rev. 114, 1709–1742.

Bansode, A., Tidona, B., von Rohr, P.R., Urakawa, A., 2013. Impact of K and Ba promoters on CO_2 hydrogenation over Cu/Al_2O_3 catalysts at high pressure. Catal. Sci. Technol. 3, 767–778.

Bobadilla, L.F., Riesco-García, J.M., Penelás-Pérez, G., Urakawa, A., 2016. Enabling continuous capture and catalytic conversion of flue gas CO_2 to syngas in one process. J. CO2 Util. 14, 106–111 .

Chen, C.-S., Cheng, W.-H., Lin, S.-S., 2000. Mechanism of CO formation in reverse water–gas shift reaction over Cu/Al_2O_3 catalyst. Catal. Lett. 68, 45–48.

Christmann, K., 1995. Some general aspects of hydrogen chemisorption on metal surfaces. Prog. Surf. Sci. 48, 15–26.

Cimino, S., Boccia, F., Lisi, L., 2020. Effect of alkali promoters (Li, Na, K) on the performance of Ru/Al_2O_3 catalysts for CO_2 capture and hydrogenation to methane. J. CO2 Util. 37, 195–203.

Conner, W.C., Falconer, J.L., 1995. Spillover in heterogeneous catalysis. Chem. Rev. 95, 759–788.

Cui, X., Kær, S.K., 2019. Thermodynamic analyses of a moderate-temperature process of carbon dioxide hydrogenation to methanol via reverse water–gas shift with in situ water removal. Ind. Eng. Chem. Res. 58, 10559–10569.

Daza, Y.A., Kuhn, J.N., 2016. CO_2 conversion by reverse water gas shift catalysis: comparison of catalysts, mechanisms and their consequences for CO_2 conversion to liquid fuels. RSC Adv. 6, 49675–49691.

Duan, Y., Luebke, D.R., Pennline, H.H., 2012. Efficient theoretical screening of solid sorbents for CO_2 capture applications. Int. J. Clean Coal Energ. 1, 1–11.

Duyar, M.S., Treviño, M.A.A., Farrauto, R.J., 2015. Dual function materials for CO_2 capture and conversion using renewable H2. Appl. Catal. B 370–376 168-169.

Ernst, K.-H., Campbell, C.T., Moretti, G., 1992. Kinetics of the reverse water-gas shift reaction over Cu(110). J. Catal. 134, 66–74.

Fernández, J.R., Garcia, S., Sanz-Pérez, E.S., 2020. CO_2 capture and utilization editorial. Ind. Eng. Chem. Res. 59, 6767–6772.

Ferretto, L., Glisenti, A., 2003. Surface acidity and basicity of a rutile powder. Chem. Mater. 15, 1181–1188.

Garcia Cortez, G., Fierro, J.L.G., Bañares, M.A., 2003. Role of potassium on the structure and activity of alumina-supported vanadium oxide catalysts for propane oxidative dehydrogenation. Catal. Today 78, 219–228.

Gordon, S., Campbell, C., 1955. Differential thermal analysis of inorganic compounds. Anal. Chem. 27, 1102–1109.

Hartman, M., Svoboda, K., Čech, B., Pohořelý, M., Šyc, M., 2019. Decomposition of Potassium Hydrogen Carbonate: thermochemistry, Kinetics, and Textural changes in solids. Ind. Eng. Chem. Res. 58, 2868–2881.

Haszeldine, R.S., Flude, S., Johnson, G., Scott, V., 2018. Negative emissions technologies and carbon capture and storage to achieve the Paris Agreement commitments. Philos. Trans. Royal Soc. A 376, 20160447.

Hu, L., Urakawa, A., 2018. Continuous CO_2 capture and reduction in one process: CO_2 methanation over unpromoted and promoted Ni/ZrO_2. J. CO2 Util. 25, 323–329.
Hyakutake, T., van Beek, W., Urakawa, A., 2016. Unravelling the nature, evolution and spatial gradients of active species and active sites in the catalyst bed of unpromoted and K/Ba-promoted Cu/Al_2O_3 during CO_2 capture-reduction. J. Mater. Chem. A 4, 6878–6885.
Jurković, D.L., Pohar, A., Dasireddy, V.D.B.C., Likozar, B., 2017. Effect of copper-based catalyst support on reverse water-gas shift reaction (RWGS) Activity for CO_2 Reduction. Chem. Eng. Technol. 40, 973–980.
Kantschewa, M., Albano, E.V., Etrtl, G., Knözinger, H., 1983. Infrared and x-ray photoelectron spectroscopy study of K_2CO_3/γ-Al_2O_3. Appl. Catal. 8, 71–84.
Keim, W., 1986. C1 chemistry: potential and developments. Pure Appl. Chem. 58, 825–832.
Kosaka, F., Liu, Y., Chen, S.-Y., Mochizuki, T., Takagi, H., Urakawa, A., et al., 2021. Enhanced activity of integrated CO_2 capture and reduction to CH_4 under pressurized conditions toward atmospheric CO_2 utilization. ACS Sustain. Chem. Eng. 9, 3452–3463.
Kosaka, F., Sasayama, T., Liu, Y., Chen, S.-Y., Mochizuki, T., Matsuoka, K., et al., 2022. Direct and continuous conversion of flue gas CO_2 into green fuels using dual function materials in a circulating fluidized bed system. Chem. Eng. J. 450, 138055.
Lahousse, C., Aboulayt, A., Maugé, F., Bachelier, J., Lavalley, J.C., 1993. Acidic and basic properties of zirconia—Alumina and zirconia—Titania mixed oxides. J. Mol. Catal. 84, 283–297.
Leclaire, J., Heldebrant, D.J., 2018. A call to (green) arms: a rallying cry for green chemistry and engineering for CO_2 capture, utilisation and storage. Green Chem. 20, 5058–5081.
Lee, J.M., Min, Y.J., Lee, K.B., Jeon, S.G., Na, J.G., Ryu, H.J., 2010. Enhancement of CO_2 sorption uptake on Hydrotalcite by Impregnation with K_2CO_3. Langmuir 26, 18788–18797.
Luo, J., Gao, F., Kim, D.H., Peden, C.H.F., 2014. Effects of potassium loading and thermal aging on K/Pt/Al_2O_3 high-temperature lean NO_x trap catalysts. Catal. Today 231, 164–172.
Marceau, E., Carrier, X., Che, M., 2009. Impregnation and Drying, Synthesis of Solid Catalysts. Wiley-VCH pp. 59-82.
Marocco Stuardi, F., MacPherson, F., Leclaire, J., 2019. Integrated CO_2 capture and utilization: a priority research direction. Curr. Opin. Green Sustain. Chem. 16, 71–76.
Mikkelsen, M., Jørgensen, M., Krebs, F.C., 2010. The teraton challenge. A review of fixation and transformation of carbon dioxide. Energy Environ. Sci. 3, 43–81.
Oliveira, E.L.G., Grande, C.A., Rodrigues, A.E., 2008. CO_2 sorption on hydrotalcite and alkali-modified (K and Cs) hydrotalcites at high temperatures. Sep. Purif. Technol. 62, 137–147.
Pinto, D., van der Bom Estadella, V., Urakawa, A., 2022. Mechanistic insights into the CO_2 capture and reduction on K-promoted Cu/Al_2O_3 by spatiotemporal operando methodologies. Catal. Sci. Technol. 12, 5349–5359.
Porosoff, M.D., Yan, B., Chen, J.G., 2016. Catalytic reduction of CO_2 by H_2 for synthesis of CO, methanol and hydrocarbons: challenges and opportunities. Energy Environ. Sci. 9, 62–73.
Rodriguez, J.A., Kim, J.Y., Hanson, J.C., Pérez, M., Frenkel, A.I., 2003. Reduction of CuO in H_2: in Situ Time-Resolved XRD Studies. Catal. Lett. 85, 247–254.
Roesch, A., Reddy, E.P., Smirniotis, P.G., 2005. Parametric Study of Cs/CaO Sorbents with respect to simulated flue gas at high temperatures. Ind. Eng. Chem. Res. 44, 6485–6490.
Rubin, E.S., Davison, J.E., Herzog, H.J., 2015. The cost of CO_2 capture and storage. Int. J. Greenh. Gas Control 40, 378–400.
Shimizu, T., Hirama, T., Hosoda, H., Kitano, K., Inagaki, M., Tejima, K., 1999. A twin fluid-bed reactor for removal of CO_2 from combustion processes. Chem. Eng. Res. Des. 77, 62–68.
Stangeland, K., Kalai, D., Li, H., Yu, Z., 2017. CO_2 Methanation: the effect of catalysts and reaction conditions. Energy Procedia 105, 2022–2027.
Udupa, M.R., 1976. Thermal decomposition of potassium nitrate in the presence of chromium(III) oxide. Thermochim. Acta 16, 231–235.
Walspurger, S., Boels, L., Cobden, P.D., Elzinga, G.D., Haije, W.G., van den Brink, R.W., 2008. The crucial role of the K^+–Aluminium Oxide Interaction in K^+-Promoted Alumina- and Hydrotalcite-based materials for CO_2 Sorption at high temperatures. ChemSusChem 1, 643–650.
Zhang, L., Song, Y., Shi, J., Shen, Q., Hu, D., Gao, Q., et al., 2022. Frontiers of CO_2 Capture and Utilization (CCU) towards Carbon Neutrality. Adv. Atmosph. Sci. 39, 1252–1270.
Zhu, M., Ge, Q., Zhu, X., 2020. Catalytic reduction of CO_2 to CO via reverse water gas shift reaction: recent advances in the design of active and selective supported metal catalysts. Trans. Tianjin Univ. 26, 172–187.